J Chem Ecol (2017) 43:1086–1096
https://doi.org/10.1007/s10886-017-0899-8

Melanization Affects the Content of Selected Elements in Parmelioid Lichens

Lorenzo Fortuna[1] · **Elena Baracchini**[2] · **Gianpiero Adami**[2] · **Mauro Tretiach**[1]

Received: 29 August 2017 / Revised: 13 October 2017 / Accepted: 26 October 2017 / Published online: 3 November 2017

Abstract Lichens belonging to Parmeliaceae are highly diversified, but most of them share an extremely conserved morpho-chemical trait: the lower cortex is heavily melanized. The adaptive value of this character is still uncertain. Melanins are ubiquitous compounds found in most organisms since they fulfil several biological functions including defense against UV radiation, oxidizing agents, microbial stress, and metal complexation. This work aims to establish whether melanization can affect the elemental content of lichen thalli. The relative abundance of macro- (Ca, K and S) and micro- (Fe, Mn and Zn) nutrients in melanized and non-melanized pseudotissues of nine species was first evaluated by a non-destructive micro-X-ray fluorescence elemental analysis on either the upper and lower cortex, and on the internal medulla, which was artificially exposed to the mechanical removal of the lower cortex. Afterwards, the total concentration of the same elements was measured in composite samples by inductively coupled plasma atomic emission spectroscopy after acidic digestion. In order to verify whether Fe and Zn are chemically bound to the melanized pseudotissues, a sequential elution experiment was performed on two species: the two-side heavily melanized *Melanelixia glabratula* and the one-side lightly melanized *Punctelia subrudecta*. The content of Fe and Zn was higher in the melanized species than in the non-melanized ones. Species deprived of their melanized lower cortex showed a sharp decrease in Fe but not in Zn, suggesting that the melanized lower cortex is involved in Fe complexation, whereas Zn is homogeneously distributed throughout the thallus.

Keywords Bioaccumulation · Fungi · Melanins · Homeostasis · Iron · Zinc

Introduction

Lichens are a stable, extracellular symbiosis between a fungus, mostly an ascomycete (the so-called mycobiont), and one or more populations of algae and/or cyanobacteria (the so-called photobionts). Since lichens lack roots and waxy cuticle, they acquire inorganic nutrients from dry and wet atmospheric depositions (Williamson et al. 2004). Selective processes led mycobionts to evolve a multi-stratified thallus, which is dorsiventral in foliose lichens, with distinct upper and lower cortices (Nash 2008): the upper cortex ensures a favourable, variable light radiance to the photobiont (Honegger 1993), whereas the lower cortex provides the attachment to the substratum. Lichen-forming ascomycetes biosynthesize in their cortices a wide spectrum of secondary metabolites of different chemical nature (Huneck and Yoshimura 1996). This varied range of secondary metabolites provides antiherbivore defense (Asplund and Gauslaa 2008; Benesperi and Tretiach 2004), protection against excess light (Gauslaa and McEvoy 2005; Solhaug and Gauslaa 1996), and/or contribute to macro- and micronutrients uptake (Hauck and Huneck 2007). The capability of certain lichen substances in over-accumulating inorganic nutrients could significantly contribute even to ecosystem functioning by providing to other organisms the needed micro-nutrient supply (Knops et al. 1996).

Electronic supplementary material The online version of this article (https://doi.org/10.1007/s10886-017-0899-8) contains supplementary material, which is available to authorized users.

✉ Mauro Tretiach
tretiach@units.it

[1] Department of Life Sciences, University of Trieste, Via L. Giorgieri 10, I-34127 Trieste, Italy

[2] Department of Chemical and Pharmaceutical Sciences, University of Trieste, Via L. Giorgieri 1, I-34127 Trieste, Italy

Most of the foliose macrolichens belonging to a highly evolved and diversified group, e.g. the family Parmeliaceae, share a common, highly conserved phenotypic trait: a well-developed lower cortex which is brown to black due to the heavy deposition of melanin-like pigments on the mycobiont cell wall (Rikkinen 1995). This trait is often present in other taxonomic groups as well, e.g. in Physciaceae and Peltigerales, but in this case species with a highly melanized lower cortex are closely related to a white, non-melanized lower cortex. The adaptive value of the melanization of the lower cortex is still unclear.

Melanins are found in most organisms of all biological kingdoms and can fulfil different functions; from the most obvious and well-known, i.e. UV-screening (Solhaug et al. 2003; Matee et al. 2016; Mafole et al. 2017), to defense against oxidising agents (Eisenman and Casadevall 2012) and biochemical threats (Pilas et al. 1988). Melanogenesis in non-lichenised ascomycetes has been related to the polyketide synthase (PKS) genes, which control the intracellular biosynthesis of the melanin monomer, 1,8-dihydroxynaphtalene (DHN) (Bell and Wheeler 1986; Muggia and Grube 2010). Opanowicz et al. (2005) detected the PKS1 paralog in both Parmeliaceae and non-lichenized ascomycetes, pointing out that some genera of Parmeliaceae form a sister clade with non-lichenized genera. The authors cautiously argued that PKS1 paralog could be involved in the production of DHN-derived melanin also in Parmeliaceae.

In non-lichenized ascomycetes, melanin monomers are extruded within the cell wall or in the extracellular medium, where their polymerization may be promoted by oxidase enzymes (Butler and Day 1998). Alternatively, polymerization is triggered by an increase in the pH, which allows autoxidation of monomers. Some authors refer to these melanins as "heterogeneous melanin" or "fungal humic acids" (Schnitzer and Neyroud 1975), since their structure is a mixture of phenols and amino acids, carbohydrates, proteins and lipids, all of which can be partially derived from other organisms (e.g. plants, bacteria, other non-lichenized fungi). Hence, fungal DHN-derived melanin structure contains a plurality of functional groups and chemical moieties (quinone, hydroquinone and semiquinone moieties), which provide many potential binding sites for metal ions (Fogarty and Tobin 1996). Whilst saprotrophic fungal DHN-derived melanins were widely studied as Cd^{2+}, Cu^{2+} and Zn^{2+} adsorbants (Fomina and Gadd 2003; Gadd and Rome 1988;), only a few studies have been focused on melanins of lichenized fungi (McLean et al. 1998; Purvis et al. 2004). Considering that (*i*) the melanized lower cortex is a highly conserved character, (*ii*) the lower cortex is not exposed to direct sun radiation, (*iii*) several metals show high chemical affinity for fungal melanins, and (*iv*) lichen-forming fungi have to provide inorganic nutrients to their photobionts in order to get the organic carbon they need (Clark et al. 2001; Palmqvist 2000), it is plausible to suppose that the melanization process of the lower cortex might be involved in the mineral uptake of lichen thalli. This hypothesis is tested here based on a thorough investigation of the relative abundance of macro- (Ca, K and S) and micro- (Fe, Mn and Zn) nutrients in melanized and non-melanized pseudotissues of nine lichens, which have been characterized by energy dispersive micro-X-ray fluorescence (ED-μXRF) and inductively coupled plasma atomic emission spectroscopy (ICP-AES), and thanks to a sequential elution experiment performed on two species with high vs. low degree of melanization.

Methods and Materials

Sample Collection and Preparation Thalli of nine foliose lichens (Table 1) were collected with a ceramic knife in four sampling sites of the Classical Karst plateau (Trieste, NE Italy). The thalli were immediately transported to the laboratory and left to rehydrate overnight by equilibration above distilled H_2O [close to 100% relative humidity (RH)] inside sealed plastic jars, at 20 °C, and then each thallus was carefully removed from the substratum under a stereomicroscope using wooden toothpicks and plastic tweezers. Debris possibly present and dead bryophytes or damaged portions of the thalli were carefully removed. The cleaned samples were left to dry out in a protected environment in dim light.

ED-μXRF Analyses In order to evaluate the relative abundance of macro- and micro-nutrients in melanised and non-melanised thalline cortical surfaces, non-destructive ED-μXRF analysis was performed on nine lobes (i.e. the outermost, lobate part of a foliose thallus) of each species (Table 1). The measurements were directly taken on the upper surface of 3 lobes (herein, the U samples), on the lower surface of further 3 lobes (herein, the L samples), and, in five species (*F. caperata, H. physodes, M. glabratula, P. borreri and P. subrudecta*), on the internal aerenchymatic layer, the so-called medulla, of the last 3 lobes (herein, the M samples), which had been subjected to the mechanical removal of the lower cortex with a ceramic blade precision cutter under a stereomicroscope (for examples, see Online Resource 1). In order to flatten the surfaces, all the lobes were humidified for 24 hr before dehydration between two layers of filter paper (APTACA, Canelli, Italy) under a load of about 1 kg. ED-μXRF measurements were conducted on a single focal spot of 1.2 × 0.1 mm^2 on each lobe using an ARTAX 200 μ-X-ray fluorescence spectrometer (Bruker Nano GmbH, Karlsruhe, Germany). The instrument was set up with the following test parameters: X-ray tube, Mo target U = 50 kV, I = 700 μA, acquisition time: 120 sec (live time), collimator: 650 μm (air environment). The examined elements were: Ca (line: Kα1 3.6923 keV), K (line: Kα1 3.3138 keV), Fe (line: Kα1 6.4052 keV), Mn (line: Kα1 5.9003 keV), S (line: Kα1 2.3095 keV) and Zn (line: Kα1 8.6372 keV). The ED-μXRF spectra (n = 78) were processed

Table 1 List of species, subdivided between Parmeliaceae and Teloschistales, ordered according to the degree of melanisation of their thallus layers

Taxon [#]	Degree of melanisation	Species	U	M		L	Datasets
Parmeliaceae							
	Two-side heavily melanised						
		Melanelixia glabratula	++	–		++	B
		Xanthoparmelia loxodes	++	–	nd	++	A
	One-side heavily melanised						
		Flavoparmelia caperata	–	–		++	B
		Hypogymnia physodes	–	–		++	B
		Punctelia borreri	–	–		++	B
	One-side lightly melanised						
		Punctelia subrudecta	–	–		+	B
Teloschistales							
	One-side heavily melanised						
		Physconia distorta	+	–	nd	++	A
	One-side lightly melanised						
		Physconia grisea	–	–	nd	+	A
	Non-melanised						
		Xanthoria parietina	–	–	nd	–	A

U, Upper cortex; M, Medulla; *L*, Lower cortex. Species are referred to datasets a, b depending on which thalline surface was analysed by ED-μXRF. A: Analysis limited to external thalline layers (U, L); B: Analysis performed on internal and external thalline layers (U, M, L), Parmeliaceae species only. ++: Heavily melanized; +: Lightly melanized; −: Non-melanized; nd: Not analysed

[#] Nomenclature according to Nimis (2016)

with ARTAX ® software to calculate by integration the area of elemental peaks (Ap) and that of the spectrum included between 2 and 10 keV (At). The relative abundance of Ca, K, Fe, Mn, S and Zn detected in each sample was then expressed as a percentage ratio between Ap and At.

In order to verify if a moiety of the investigated elements was associated to the soluble fraction, nine samples of *F. caperata* were prepared as described before, after washing them separately four times for 20, 15, 10 and 5 min respectively in 10 ml of distilled water.

ICP-AES Analyses Total elemental compositions were assessed by ICP-AES with a PerkinElmer Optima 8000 equipped with autosampler S10 in composite samples of the single species respectively formed by the intact lobes (U plus L samples: herein, the U + L samples) and the lower-cortex-deprived M samples (herein, the M' samples). This material was digested in polypropylene flasks containing 1 mL HNO_3 69% (Trace Select, Fluka Analytical), 100 μL H_2O_2 30% (Trace Select, Sigma Aldrich) and 25 μL HF 48% (Trace Select, Sigma Aldrich) following a three-step heating program in "bain-marie" up to 70 °C in a digestion block (PerkinElmer SPB 100–12). After mineralization, 100 μl of 6% boric acid solution (Trace Select, Sigma Aldrich) was added and then the solutions were diluted to a final volume of 10 ml with MilliQ water.

Element concentrations were measured using a calibration curve, obtained by dilution of Ca, K, Fe, Mn and Zn standard solutions (SPECTRASCAN ®, Teknolab) for ICP-AES analyses. The limit of detection (LOD) at the operative wavelength for each element was: 0.050 mg/L for Ca at 317.933 nm and K at 766.490 nm, 0.030 mg/L for Fe at 238.204 nm, 0.020 mg/L for Mn at 257.610 nm and Zn at 206.200 nm. The repeatability of the measurements as relative standard deviation (RSD%) was always lower than 5%.

Sequential Elution Technique (SET) In order to evaluate whether Fe and Zn are bound to the melanized hyphae, a SET experiment was carried out on two species: the two-side heavily melanized *M. glabratula* and the one-side lightly melanized *P. subrudecta*, selected for their uniform cell wall chemistry (Krog 1982; Blanco et al. 2004; Smith et al. 2009). SET protocols call for the use of a well-defined chemical compound to extract the extracellular fraction of a specific element. Several studies provide detailed information regarding Zn extraction by NiCl, EDTA or Na_2-EDTA whereas Fe extraction was discussed in fewer studies, based on the use of EDTA or Na_2-EDTA (Pérez-Llamazares et al. 2011). Since EDTA can cause the efflux of intracellular elements by cell membrane damage, in this work the less reactive Na_2-EDTA was chosen as extractant for both Fe and Zn.

Five samples (about 100 mg dry mass each) of *M. glabratula* and *P. subrudecta*, taken from the same thalli analysed by ED-μXRF and ICP-AES, were processed. After selection, the material was stored at 98% RH (as above) to re-establish the

permeability membrane integrity (Buck and Brown 1979) and treated following Branquinho and Brown (1994) with the modifications proposed by Pérez-Llamazares et al. (2011). The intercellular fraction was removed by shaking the samples twice in 10 ml of double distilled water for 30 and 40 min, respectively. Afterwards, the samples were shaken in 10 ml of 20 mM Na_2-EDTA (Sigma Aldrich) for 40 min, then the solution was replaced and the samples were incubated at room temperature for 30 min. The two Na_2-EDTA solutions were combined for analysis to obtain the elemental content of the extracellular fraction. The intracellular fractions were extracted by shaking the samples in 10 mL of 1 M HNO_3 (Carlo Erba) for 2 hr at about. 15 °C. The samples were then dried at 45 °C for 36 hr and weighed to calculate the mass of the cell walls.

In order to evaluate the residual fraction, the samples were digested with a mixture of 2.63 ml of 69% HNO_3, 380 μl of 30% H_2O_2 and 75 μl of 48% HF in Teflon pressure vessels by means of a microwave-assisted digestion system (Multiwave PRO, Anton Paar) following a heating program in accordance with the standard procedure EPA-3052 (U.S. Environmental Protection Agency 1996). After mineralization, 380 μl of 6% boric acid solution was added and the solutions were heated again and diluted to a final volume of 15 ml with MilliQ water. After each treatment, about 10 ml of the elution was sampled, filtered with a 0.45 μm pre-filter (GHP Acrodisc, Pall Corporation) and analyzed by ICP-AES to measure the concentration of K, Fe and Zn. Five untreated samples of both species were ground in an agate mortar with 20 ml of liquid nitrogen and then mineralized as described above. The total concentrations of K, Fe and Zn measured in these samples were compared with the sum of the four fractions.

Statistical Analyses The ED-μXRF data were organized in two datasets, namely A and B, the former comprised of the nine species analysed at the cortical level, and the latter including only the five species that could also be analysed at the medullary level (see Table 1). Dataset A was implemented to compare the differences in terms of elemental relative abundance between upper and lower cortex (i.e. U and L samples) with the *Mann-Whitney U test for unpaired samples*. Dataset B was submitted to *Principal Component Analysis* (PCA) in order to investigate specific relations among groups of elements, external and internal layers (i.e. U, L and M samples), and degree of melanization. Furthermore, the specific relations among the abundance of the elements were evaluated by Pearson's *r* for each thalline layer, and *one-way ANOVA* and *LSD's post-hoc* test were used to evaluate the statistical differences in terms of relative abundance of elements among thalline layers.

The ED-μXRF data of Parmeliaceae (see Table 1) were correlated to the respective ICP-AES data. For example, the U and L samples were coupled with the respective U + L samples, and the M samples were coupled with the respective M' samples. These comparisons were repeated using the average value of each thalline surface as well as the average value obtained from all the measurements.

The element concentrations measured in the SET experiment were compared by *factorial ANOVA* considering species and fractions as categorical factors. The statistical differences among the fractions of each species and between the same fraction of the two species were evaluated by *LSD's post-hoc* test.

Results

ED-μXRF Analyses In all the species the relative abundance of Ca, K and Fe (Table 2) was on average one to two order of magnitude higher than that of Mn, S and Zn. The species belonging to the Parmeliaceae showed on average a lower abundance of K and Zn than those belonging to the order Teloschistales (*Xanthoria parietina* at first, then *Ph. grisea* and *Ph. distorta*). On the other hand, the spectra of Parmeliaceae were characterised by a Ca peak corresponding up to 85% of the whole spectrum area. Therefore, the relative abundance of other elements was highly and negatively correlated with that of Ca (Table 3). Despite this, the PCA based on dataset B reveals a clear relationship among groups of elements, thalline surfaces and degree of melanization (Fig. 1): K and S were strictly associated with the upper cortex, Ca with the medulla and Fe with the melanized lower cortex; conversely, Mn and Zn were associated with both the upper and the lower cortex.

The outcomes of *one-way ANOVAs* analyses (Table 2; *F-statistic* are reported in Online Resource 2) show that on average the upper cortex of all the species contained more K, Mn and S than the other thalline surfaces. In particular, the U samples of *F. caperata*, *P. subrudecta* and *M. glabratula* were characterised by a significant high relative abundance of K and S, K, and Mn and S, respectively. All species showed an enrichment of Ca in M samples; these samples were statistically different from U samples of *F. caperata* and *P. subrudecta*. On the contrary, Zn did not differ among the U, M and L samples of all these species. When melanised, the lower surfaces and – to a lesser extent – the upper ones contained Fe for the most part (Fig. 2). In fact, the removal of the melanised lower cortex caused a sharp decrease of Fe, as confirmed by the statistical differences between the M and L samples of *F. caperata*, *H. physodes* and *P. subrudecta* (Table 2).

The washing of *F. caperata* samples in distilled water did not affect the intra-thalline element distribution (Table 2).

The comparisons made by *Mann-Whitney U test for unpaired samples* between U and L samples of those species whose medulla could not be analyzed (dataset B, see Table 1) revealed a significantly higher relative abundance of Ca in the upper surface of *Ph. distorta* and in the lower surface of *X. loxodes*. The upper melanized surface of *X. loxodes* was significantly enriched with both Fe and Mn whereas the lower melanized surface of *Ph. grisea* was significantly enriched with K, Fe, S and Zn (Table 2).

Table 2 Average relative abundances of Ca, Fe, K, Mn, S and Zn measured by ED-μXRF on the thalline layers of U, M and L samples

Taxon	Sample	Ca	Fe	K	Mn	S	Zn
Parmeliaceae							
M. glabratula							
	U	0.618 ± 0.012	0.048 ± 0.042	0.141 ± 0.044	0.008 ± 0.002***b***	0.015 ± 0.004***b***	0.021 ± 0.003
	M	0.685 ± 0.064	0.039 ± 0.022	0.092 ± 0.030	0.005 ± 0.001***a***	0.010 ± 0.003***ab***	0.020 ± 0.006
	L	0.646 ± 0.051	0.093 ± 0.039	0.087 ± 0.015	0.005 ± 0.002***a***	0.007 ± 0.001***a***	0.021 ± 0.004
X. loxodes							
	U	0.636 ± 0.110	0.147 ± 0.097*	0.045 ± 0.009	0.002 ± 0.001*	0.003 ± 0.001	0.013 ± 0.004
	M	nd	nd	nd	nd	nd	nd
	L	0.749 ± 0.012*	0.070 ± 0.011	0.032 ± 0.007	0.002 ± 0.001	0.002 ± 0.001	0.008 ± 0.003
F. caperata							
	U	0.725 ± 0.011***a***	0.021 ± 0.008***ab***	0.108 ± 0.004***c***	0.003 ± 0.001	0.006 ± 0.001***b***	0.009 ± 0.002
	M	0.779 ± 0.026***b***	0.006 ± 0.004***a***	0.075 ± 0.021***b***	0.002 ± 0.001	0.005 ± 0.002***b***	0.008 ± 0.004
	L	0.783 ± 0.022***b***	0.041 ± 0.016***b***	0.035 ± 0.007***a***	0.003 ± 0.002	0.002 ± 0.001***a***	0.005 ± 0.002
F. caperata (w)							
	U	0.583 ± 0.137***a***	0.021 ± 0.011***ab***	0.231 ± 0.111***b***	0.006 ± 0.001***c***	0.015 ± 0.007***b***	0.020 ± 0.014
	M	0.766 ± 0.043***b***	0.007 ± 0.001***a***	0.071 ± 0.022***a***	0.002 ± 0.001***a***	0.007 ± 0.004***ab***	0.014 ± 0.005
	L	0.756 ± 0.019***b***	0.044 ± 0.011***b***	0.051 ± 0.011***a***	0.003 ± 0.001***b***	0.004 ± 0.001***a***	0.011 ± 0.002
H. physodes							
	U	0.675 ± 0.097	0.046 ± 0.008***ab***	0.090 ± 0.065	0.006 ± 0.003	0.008 ± 0.007	0.021 ± 0.010
	M	0.817 ± 0.022	0.009 ± 0.001***a***	0.029 ± 0.018	0.003 ± 0.002	0.002 ± 0.001	0.009 ± 0.004
	L	0.534 ± 0.242	0.229 ± 0.159***b***	0.060 ± 0.059	0.005 ± 0.002	0.005 ± 0.005	0.020 ± 0.019
P. borreri							
	U	0.676 ± 0.019	0.044 ± 0.022	0.124 ± 0.010	0.004 ± 0.001	0.007 ± 0.001	0.009 ± 0.003
	M	0.736 ± 0.059	0.015 ± 0.008	0.108 ± 0.045	0.002 ± 0.002	0.009 ± 0.006	0.005 ± 0.003
	L	0.691 ± 0.096	0.057 ± 0.039	0.099 ± 0.044	0.004 ± 0.003	0.005 ± 0.003	0.006 ± 0.003
P. subrudecta							
	U	0.697 ± 0.084***a***	0.019 ± 0.005***b***	0.121 ± 0.061***b***	0.006 ± 0.002	0.004 ± 0.004	0.005 ± 0.002
	M	0.841 ± 0.003***b***	0.003 ± 0.002***a***	0.026 ± 0.004***a***	0.003 ± 0.001	0.001 ± 0.001	0.003 ± 0.001
	L	0.770 ± 0.034***ab***	0.020 ± 0.009***b***	0.061 ± 0.027***ab***	0.005 ± 0.004	0.002 ± 0.001	0.004 ± 0.002
Teloschistales							
Ph. distorta							
	U	0.645 ± 0.180	0.033 ± 0.027	0.140 ± 0.111	0.003 ± 0.003	0.004 ± 0.004	0.043 ± 0.034
	M	nd	nd	nd	nd	nd	nd
	L	0.526 ± 0.093	0.122 ± 0.146	0.161 ± 0.080	0.007 ± 0.004	0.005 ± 0.001	0.035 ± 0.013
Ph. grisea							
	U	0.733 ± 0.013*	0.037 ± 0.010	0.091 ± 0.021	0.002 ± 0.001	0.003 ± 0.001	0.010 ± 0.004
	M	nd	nd	nd	nd	nd	nd
	L	0.458 ± 0.113	0.122 ± 0.030*	0.224 ± 0.074*	0.004 ± 0.003	0.009 ± 0.005*	0.029 ± 0.009*
X. parietina							
	U	0.204 ± 0.014	0.085 ± 0.067	0.438 ± 0.067	0.010 ± 0.004	0.080 ± 0.010	0.025 ± 0.008
	M	nd	nd	nd	nd	nd	nd
	L	0.227 ± 0.034	0.108 ± 0.056	0.372 ± 0.022	0.014 ± 0.001	0.075 ± 0.022	0.037 ± 0.009

Species ordered as in Table 1. *nd*, Not analyzed; *W,* Water-washed

Different letters indicate significant differences as calculated by *one-way ANOVA* and *LSD*'s post-hoc tests ($P < 0.05$) for the species B of Table 1 (F values are reported in Online Resource 2). *: significant differences ($P < 0.05$) between U and L samples as calculated by *Mann-Whitney U test* for the species A of Table 1. Values are reported as mean ± standard deviation; $n = 3$

Table 3 Pearson's correlation coefficients (R) calculated among relative abundances of elements measured by ED-μXRF in each thalline layer (U, M and L samples) for the species B of Table 1

	Ca	K	Fe	S	Mn	Zn
U						
Ca						
K	−0.814***					
Fe	−0.150	−0.407				
S	−0.850***	0.849***	−0.220			
Mn	−0.561*	0.416	−0.103	0.670**		
Zn	−0.819***	0.563*	0.216	0.809***	0.558*	
M						
Ca						
K	−0.873***					
Fe	−0.837***	0.537*				
S	−0.929***	0.917***	0.630**			
Mn	−0.571*	0.341	0.661**	0.457		
Zn	−0.693**	0.353	0.704**	0.562*	0.543*	
L						
Ca						
K	−0.600**					
Fe	−0.939***	0.297				
S	−0.697**	0.817***	0.471**			
Mn	−0.548**	0.538**	0.426	0.327		
Zn	−0.824***	0.525*	0.727**	0.788***	0.372	

Levels of significance: *** for $P \leq 0.001$; ** for $0.001 < P \leq 0.01$; * for $0.01 < P \leq 0.05$

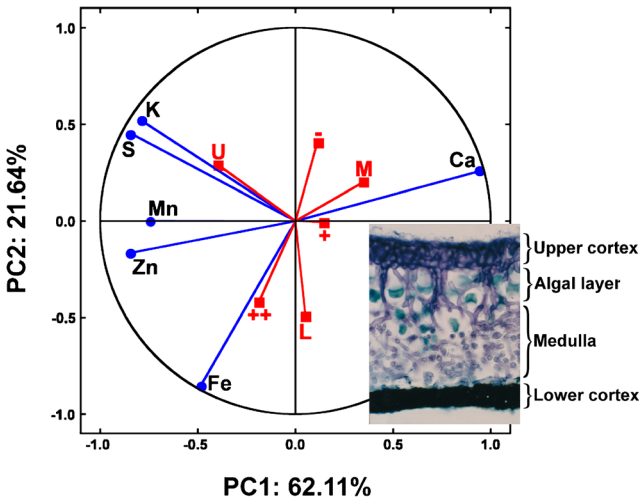

Fig. 1 The projection of the variables on the factor-plane for the relative abundance of Ca, K, Fe, Mn, S and Zn measured by ED-μXRF in U, M and L samples of species B in Table 1. The thalline surfaces and their degree of melanization (see Table 1) were treated as supplementary variables. U: upper cortex; M: medulla; L: lower cortex. ++: heavily melanized surfaces; +: lightly melanized surfaces; −: non-melanized surfaces. The frame on the right shows a transversal section of a thallus of *Punctelia borreri* after staining with Toluidine blue O 0.05% in acetate buffer pH 4.4 as a metachromatic stain

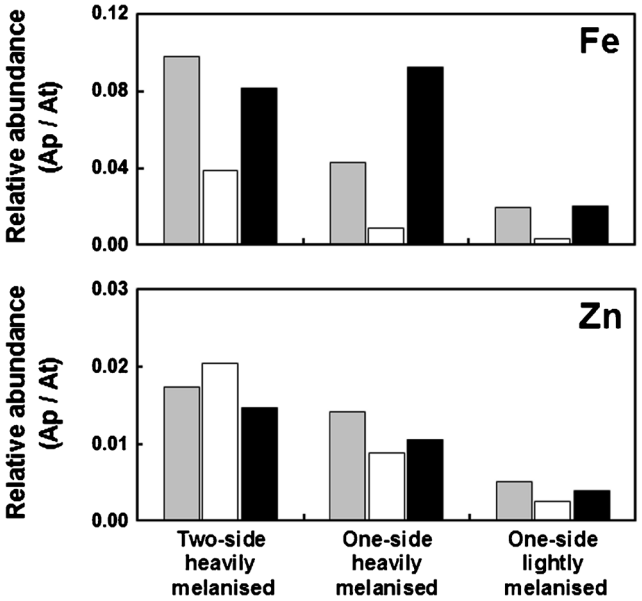

Fig. 2 The average of Fe and Zn relative abundances (upper and lower panel, respectively) measured by ED-μXRF in U (grey bars), M (white bars), L (black bars) samples of two-side and one-side heavily melanized and one-side lightly melanized Parmeliaceae species. The vertical axis reports the ratio between the area of element peak (Ap) and that of the ED-μXRF spectrum between 2 and 10 keV (At). See Table 1 for species description

ICP-AES Analyses and Reliability of ED-μXRF Measurements The quantitative ICP-AES analyses showed that Fe and Zn were the highest in the Parmeliaceae species classified as two-side heavily melanized and one-side heavily melanized whereas the lowest concentrations were observed in the one-side lightly melanized species (Fig. 3). The samples U + L and M' had similar concentrations of Ca, K, Mn and Zn, except for Fe, as the removal of the lower cortex heavily affected the concentration of this element (Table 4).

The elemental composition measured in U + L samples of Parmeliaceae and Teloschistales differ significantly, because on average the former had higher contents of Ca, Fe, Mn and Zn. Based on these results, the comparison between ICP-AES and ED-μXRF data were restricted to Parmaliaceae only (Table 5). The total concentrations of K and Mn measured in U + L and M' samples by ICP-AES were not correlated with their respective ED-μXRF measurements or with the average values. As far as Ca is concerned, only the ED-μXRF measurements performed on the medulla were significantly correlated with total concentrations measured in the same samples (M'; $P < 0.01$). On the contrary, the total concentrations of Zn measured in U + L and M' samples were highly correlated with the respective ED-μXRF data (Table 5). As for Fe the correlations between ED-μXRF and ICP-AES data were significant for both U vs U + L samples and for M vs M' samples (Table 5). Although the L samples had on average a high relative abundance of Fe with respect to both U and M samples, the correlation between L and U + L samples was

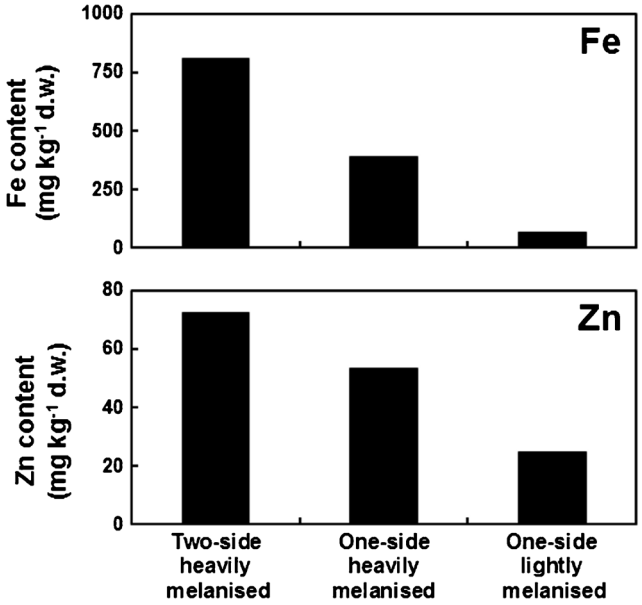

Fig. 3 The average concentrations of Fe and Zn (upper and lower panel, respectively) measured by ICP-AES in U + L samples of two-side and one-side heavily melanized and one-side lightly melanized Parmeliaceae species. See Table 1 for species description

significant only when the data of *X. loxodes* were excluded. In fact, Fe relative abundance evaluated by ED-μXRF on the lower surface of *X. loxodes* was highly underestimated in comparison to the total Fe concentration measured by ICP-AES (Fig. 4).

Sequential Elution Technique (SET) The K, Fe and Zn content measured in the intercellular, extracellular, intracellular and residual fraction of *M. glabratula* and *P. subrudecta* are given as average values in Fig. 5. The trends of the concentrations of Fe and Zn measured in the four fractions were similar in both species showing an intercellular content of Fe and Zn lower than their limit of detection. The highest contents of Fe and Zn were respectively observed in the residual and intracellular fraction of both species. In the mutual comparison, the highly two-side heavily melanised *M. glabratula* contained more Fe and Zn than the one-side lightly melanized *P. subrudecta.*

Discussion

Richardson et al. (1995) and Aslan et al. (2006) have already employed X-ray fluorescence techniques with the aim of estimating the elemental composition of lichens, but in those studies the samples were manipulated as fine powders or pellets. Whilst the pulverization of lichen material ensures high accuracy, it does not allow to discern possible differences in the elemental content of thalline layers. In order to verify the accuracy of our ED-μXRF analyses on intact thalline surfaces, we selected a set of elements (Ca, K, Mn and S) that have well known intrathalline distribution patterns. K, Mn and S are concentrated in the upper cortex and in the algal layer, mostly in the intracellular fraction (Godinho et al. 2009; Paul et al. 2003). Although the relative abundance of both K and Mn was higher in U samples than in the other thalline layers, it was not related to the total concentrations measured by ICP-AES on composite samples (i.e. U + L and M' samples; see Table 5). The lack of congruence between the two analytical techniques suggests that ED-μXRF data acquired from intact lobes

Table 4 Total concentration (mg/kg) of Ca, K, Fe, Mn and Zn measured by ICP-AES on composite samples of intact lobes (U + L) and lower-cortex-deprived lobes (M')

Taxon	Ca		K		Fe		Mn		Zn	
	U + L	M'	U + L	M'	U + L	M'	U + L	M'	U + L	M'
Parmeliaceae										
M. glabratula	16,442	21,059	3105	2925	409.8	151.2	21.2	20.0	64.0	72.3
X. loxodes	59,566	nd	4634	nd	1212.2	nd	34.1	nd	79.6	nd
F. caperata	30,605	23,563	4732	5082	306.5	11.6	15.3	15.0	40.4	44.5
F. caperata (w)	30,234	23,083	4955	3839	322.6	< LOD	16.6	11.3	65.7	70.2
H. physodes	34,436	32,110	3373	2981	687.5	114.5	24.8	19.8	69.1	73.8
P. borreri	22,157	28,840	4552	4336	244.4	63.9	17.5	13.0	32.2	25.7
P. subrudecta	23,204	46,803	4292	4335	183.0	65.9	37.4	42.0	29.1	24.7
Teloschistales										
Ph. distorta	25,999	nd	6209	nd	152.5	nd	12.9	nd	76.5	nd
Ph. grisea	9733	nd	5688	nd	222.9	nd	12.6	nd	30.3	nd
X. parietina	2371	nd	3772	nd	183.0	nd	8.9	nd	36.9	nd

Species are ordered as in Table 1. *nd* Not analyzed; W, Water-washed; *LOD*, Limit of detection

Table 5 Pearson's r calculated between ED-μXRF and ICP-AES data of Parmeliaceae species

	Single values			Average for each surface			Average of U, M and L samples	
	a	b	c	d	e	f	g	h
Ca	−0.061	0.641**	0.101	−0.111	0.772°	0.143	0.206	0.518
Fe	0.712***	0.610**	0.300	0.972***	0.729	0.386	0.947**	0.686
K	0.193	0.116	−0.308	0.255	0.142	−0.451	0.286	−0.039
Mn	−0.065	0.187	0.070	−0.084	0.242	0.113	0.449	0.424
Zn	0.560**	0.702**	0.440*	0.787*	0.808°	0.599	0.920**	0.925**

Levels of significance: *** for $P \leq 0.001$; ** for $0.001 < P \leq 0.01$; * for $0.01 < P \leq 0.05$; ° for $0.05 < P \leq 0.1$

a: U VS U + L samples; b: M VS M' samples; c: L VS U + L samples; d: average values of U vs U + L samples; e: average values of M samples VS M'; f: average of L samples vs U + L; g: average of U, L and M samples vs U + L samples; h: average of U, L and M samples vs M' samples

cannot be used in the estimation of the total concentration of K and Mn. Nevertheless, comparing the *one-way ANOVAs* results (Table 2) with those of the SET experiment (Fig. 5), also considering the significant correlation with S (Table 3), our ED-μXRF data confirm that both elements are mainly stored in the upper portion of lichen thalli, in accordance with the results of the above-mentioned studies.

Data on Ca can be used to verify the ED-μXRF data, because many lichens form Ca-oxalates deposits in the medulla, in the upper cortex or both, up to 6% of their dry mass (Giordani et al. 2003). In our case, Ca contents measured by ED-μXRF and ICP-AES on the same samples of Parmeliaceae were significantly correlated ($P < 0.01$), highlighting a more than satisfactory accuracy of the ED-μXRF analyses when performed on M samples. Similarly, the U samples of *Physconia* species revealed an enrichment of Ca in comparison to the L samples (Table 2) because the upper cortex is covered by Ca-oxalate crystals, forming the so-called *pruina* (Wadsten and Moberg 1985). At the same time, we also observed agreement between ED-μXRF and ICP-AES data concerning the content of Fe and Zn (Table 5). Therefore, it is possible to assert that the ED-μXRF technique provided reliable data, particularly for those elements that mostly occur extracellularly or in the residual fraction (Ca, Zn and Fe), even though the measurements were performed on intact lichen surfaces.

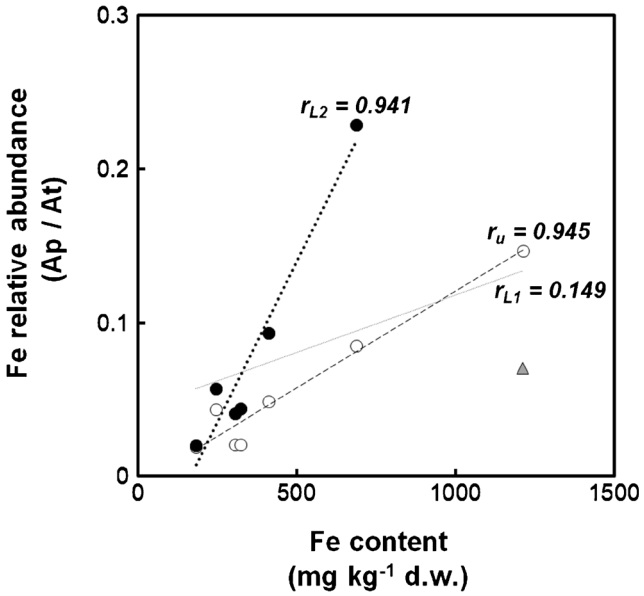

Fig. 4 The correlations among Fe content measured by ICP-AES in U + L samples and average Fe relative abundance detected by ED-μXRF in U (white dots) and L (black dots plus grey triangle) samples of Parmeliaceae species. r_{L1}, r_{L2} and r_U: Person's *r* respectively calculated for L samples, L samples excluding *X. loxodes* samples (grey triangle) and U samples

In our study, the removal of melanized lower cortex evidently affected only Fe content whereas the degree of melanization seems to influence the total Zn content (Fig. 2; Fig. 3). In fact, both the ED-μXRF and ICP-AES analyses clearly showed that the two-side heavily melanized species (*M. glabratula* and *X. loxodes*) have higher Fe and Zn contents than the one-side heavily melanized (*F. caperata*, *H. physodes*, *P. borreri*) and the one-side lightly melanized (*P. subrudecta*) species (Fig. 3). Nevertheless, the patterns of intra-thalline distribution of Fe and Zn are different. Zn showed similar relative concentrations in the three thalline surfaces (Fig. 2) investigated by ED-μXRF, whereas Fe was mainly concentrated in the external thalline surfaces, especially in the lower cortex (Fig. 2). In all the species, the removal of the lower cortex did not affect the total concentration of Zn. The similar concentrations between U + L and M' samples is consistent with the observation that Zn species are highly water-soluble and thus they can spread through the thallus, especially during wet periods. Through SET, Zn was found to be mainly associated to the intracellular fraction, which was significantly higher in the two-side heavily melanized *M. glabratula* than in the one-side lightly melanized *P. subrudecta* (Fig. 5). These results agree with previous work showing that Zn is mainly stored in the intracellular fraction (Mikhailova and Sharunova 2008) and can be translocated within the thallus (Goyal and Seaward 1982). This leads us to suppose that melanins could effectively improve Zn retention in the extracellular fraction of the melanized thalline surface(s), thus increasing the intracellular

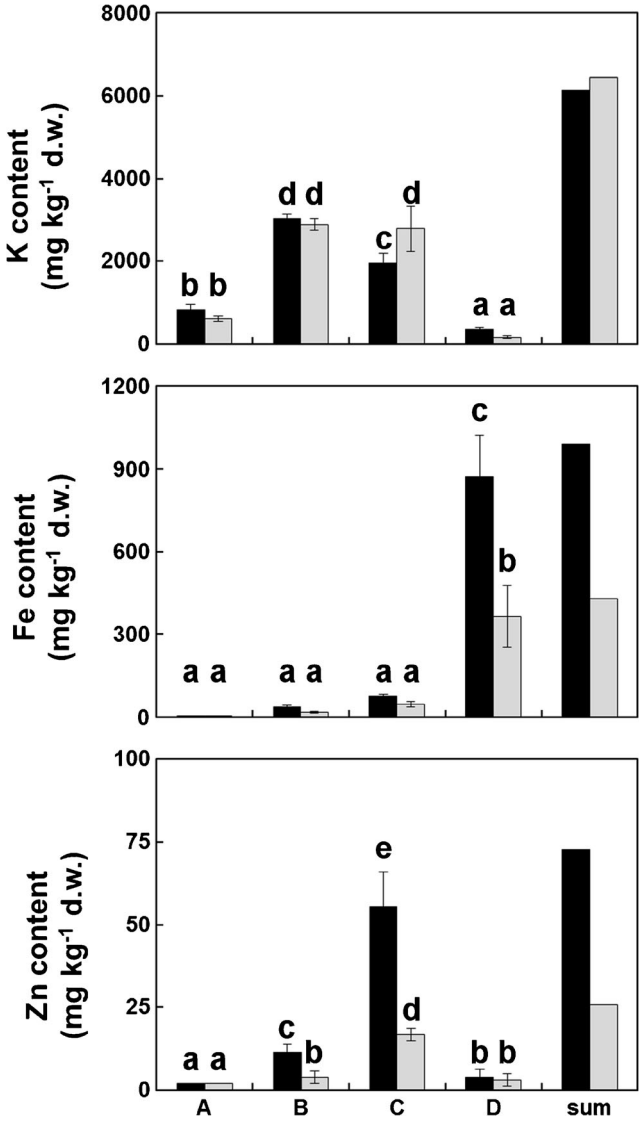

Fig. 5 The average concentrations of K, Fe and Zn (upper, middle and lower panel, respectively) measured in the intercellular (A), extracellular (B), intracellular (C) and residual fraction (D) of *Melanelixia glabratula* (black bars) and *Punctelia subrudecta* (grey bars) samples. Sum: sum of the 4 fractions. Different letters refer to statistical differences among fractions of both species for each element (LSD's Fisher post-hoc; $P < 0.05$), $n = 5$

fraction, not only of the cells close to the melanized cortical layers but of the whole thallus. On the other hand, all species showed a significant decrease in Fe when the samples were deprived of their lower surface, based on measurements with either ED-μXRF or ICP-AES. Interestingly, this result is confirmed by an unpublished work by Andreussi (personal communication) carried out by synchrotron radiation X-Ray fluorescence spectrometry, which claims that the highest relative concentration (79.2%) of Fe along the vertical thalline profile of *F. caperata* actually occurs in the lower cortex.

In terrestrial environment, Fe mostly occurs as ferric-(oxy)hydroxides rather than as the free cation (Fe^{3+} and Fe^{2+}). Our samples were collected in the Classical Karst, an environment characterised by dry, shallow (xero-)rendzina soils (Poldini 1989) that are highly enriched with several species of Al and Fe-(oxy)hydroxide (e.g. bauxite, goethite, hematite, limonite), the so-called "Terra Rossa". The major supply of Fe for epiphytic lichens collected in the Classical Karst is related to terrigenous particulate matter (PM) (Nimis et al. 2001). Terrigenous PM is mainly accumulated on the external surfaces and to a lesser extent in the medulla (Bargagli and Mikhailova 2002), where it can remain entrapped for long periods while it is dissolved by organic acids (Adamo et al. 1997), causing the release of metal ions and even inducing the neoformation and precipitation of several minerals (e.g. Garty and Garty-Spitz 2011). Hence, the considerable accumulation of terrigenous PM in the lower surfaces might explain the dramatic decrease of Fe content for those samples whose lower cortex was removed. Moreover, Fe content measured by both techniques in washed vs. unwashed samples of *F. caperata* was similar (Table 2; Table 4), confirming that this element is not available in a soluble form, and is unlikely to be removed by solubilization.

Although the relationship between melanized surfaces and Fe content seems to stem from the accumulation of terrigenous PM on the external thalline surfaces, other authors observed a strong chemical affinity of Fe for melanins of free-living and lichenized fungi, based on electron spin resonance (Saiz-Jimenez and Shafizadeh 1984; Senesi et al. 1987), electron microprobe analysis (Purvis et al. 2004) and colorimetric method (Rinino et al. 2005).

As already described for saprotrophic ascomycetes, lichenized ascomycetes could synthesize DHN-derived melanins in extracellular medium (Chowdhury et al. 2017; Purvis and Pawlik-Skowrońska 2008). During this process, either organic molecules produced by the surrounding epiphytic community and airborne materials can be included in the three-dimensional melanin structure. The structure of melanins is found to be highly heterogeneous but quite similar to that of humic-like substances, since both have high concentration of carboxyl, phenolic, hydroxyl, and amine groups that provide many potential binding sites for metal ions (Felix et al. 1978; Tian et al. 2003). Considering that in terrestrial environment Fe is not available as a free cation, it is possible to assume that melanin directly entraps Fe-(oxy)hydroxides rather than Fe^{3+}. According to this hypothesis, Schwertmann (1966) demonstrated that the anionic groups of organic matter have an inhibitory effect on the crystallization of amorphous Fe-hydroxides. Moreover, Cesco et al. (2000) showed that water–extractable humic substances are able to increase the amount of Fe present in the soil solution, possibly by forming mobile complexes with the micronutrient.

Regarding the role of melanins in Fe intracellular accumulation, De Luca and Wood (2000) suggested that fungal melanins can stimulate the reduction of Fe^{3+} to Fe^{2+} through a

passive process of electron exchange so as to regulate the intracellular Fe uptake by a Fe^{2+} specific trans-membrane carrier. Although our ED-μXRF and ICP-AES data could be in agreement with this, the results of our SET experiment pointed out that in both species almost all Fe content was in the residual fraction rather than in the intracellular fraction or chemically bound to the melanised cell wall as an exchangeable cation. However, since the difference between the intracellular fraction of *M. glabratula* and *P. subrudecta* was very low (3%), and the relative abundance of Fe in their lower surface (heavily vs lightly melanized) is different (respectively, 0.09 vs. 0.02), it can be assumed that the degree of melanization does not influence the intracellular Fe content.

Although Fe was not extractable by Na_2-EDTA treatment, there is evidence that both two-sided and one-sided highly melanized species are more Fe-enriched than the one-side lightly melanized species. This leads us to propose that melanins could improve soil particulate retention when the soil is rich in Fe-(oxy)hydroxides. Therefore, melanized thalline surfaces might act as a reservoir pool of Fe to be assimilated by the mycobiont at a later stage. In addition, this Fe reservoir pool might be important not only for lichen nourishment but also for the surrounding epiphytic community, since, as it is well-known, lichens are involved in forest nutrient cycling at the canopy level (Knops et al. 1991). In forest ecosystems, Fe is five times more concentrated in lichen thalli than in the canopy leaves (Loppi et al. 1997) and is 1000 times more concentrated than in the stemflow (Hauck and Runge 2002). This means that, especially when melanized, lichens could influence the forest Fe cycle between canopy and soil by retaining Fe-rich dry depositions (e.g. dust and soil particulate).

Although our findings suggested that melanins promote the Fe species retention, the biological mechanisms involved in the provision of bioavailable Fe species from the Fe-(oxy)hydroxides-melanin system remains unknown. It is known that the dissolution of pedogenetic Fe-hydroxides is promoted either by fungal and bacterial siderophores. To date, siderophore production has never been investigated in Parmeliaceae or in other lichen-forming fungi (Haselwandter and Winkelmann 2007). However, Swamy et al. (2016) have recently isolated lichen-inhabiting bacteria belonging to genus *Enterobacter*, which can produce siderophores.

In conclusion, our study provides analytical evidence to support the hypothesis that in parmelioid lichens the external melanized thalline surfaces influence the thallus content of Zn and are enriched in Fe. Considering the strong affinity of Fe for fungal melanins and the low bioavailability of Fe cations in terrestrial environment, the Fe(oxy)hydroxides-melanin complexes that may be present in the melanized pseudotissues might serve as a Fe reservoir pool for the provision of this essential micronutrient to the cells of both symbionts. However, alternative biological functions of melanins, only hinted at in the introduction of this work, should also be thoroughly tested.

Acknowledgments The Regional Centre of Cataloguing and Restoration of Cultural Heritage of Friuli Venezia Giulia (Udine, Italy) is thanked for providing ED-μXRF access. We thank Jessica Di Sarro and Federica Polo for their valuable work in samples analysis.

References

Adamo P, Colombo C, Violante P (1997) Iron oxides and hydroxides in the weathering interface between *Stereocaulon vesuvianum* and volcanic rock. Clay Miner 32:453–461

Aslan A, Budak G, Tıraşoğlu E, Karabulut A (2006) Determination of elements in some lichens growing in Giresun and Ordu province (Turkey) using energy dispersive X-ray fluorescence spectrometry. J Quant Spectrosc Radiat Transf 97:10–19

Asplund J, Gauslaa Y (2008) Mollusc grazing limits growth and early development of the old forest lichen *Lobaria pulmonaria* in broadleaved deciduous forests. Oecologia 155:93–99

Bargagli R, Mikhailova I (2002) Accumulation of inorganic contaminants. In: Nimis PL, Scheidegger C, Wolseley P (eds) Monitoring with lichens - monitoring lichens. Springer Science and Business Media, Dordrecht, pp 65–84

Bell AA, Wheeler MH (1986) Biosynthesis and functions of fungal melanins. Annu Rev Phytopathol 24:411–451

Benesperi R, Tretiach M (2004) Differential land snail damage to selected species of the lichen genus *Peltigera*. Biochem Syst Ecol 32:127–138

Blanco O, Crespo A, Divakar PK, Esslinger TL, Hawksworth DL, Lumbsch HT (2004) *Melanelixia* and *Melanohalea*, two new genera segregated from *Melanelia* (Parmeliaceae) based on molecular and morphological data. Mycol Res 108:873–884

Branquinho C, Brown DH (1994) A method for studying the cellular location of lead in lichens. Lichenologist 26:83–90

Buck GW, Brown DH (1979) The effect of desiccation on cation location in lichens. Ann Bot 44:265–277

Butler MJ, Day AW (1998) Fungal melanins: a review. Can J Microbiol 44:1115–1136

Cesco S, Römheld V, Varanini Z, Pinton R (2000) Solubilization of iron by water extractable humic substances. J Plant Nutr Soil Sc 163: 285–290

Chowdhury DP, Solhaug KA, Gauslaa Y (2017) Ultraviolet radiation reduces lichen growth rates. Symbiosis 73:27–34

Clark BM, Clair LLS, Mangelson NF, Rees LB, Grant PG, Bench GS (2001) Characterization of mycobiont adaptations in the foliose lichen *Xanthoparmelia chlorochroa* (Parmeliaceae). Am J Bot 88: 1742–1749

De Luca NG, Wood PM (2000) Iron uptake by fungi: contrasted mechanisms with internal or external reduction. Adv Microb Physiol 43: 39–74

Eisenman HC, Casadevall A (2012) Synthesis and assembly of fungal melanin. Appl Microbiol Biotechnol 93:931–940

Felix CC, Hyde JS, Sarna T, Sealy RC (1978) Interactions of melanin with metal ions. Electron spin resonance evidence for chelate complexes of metal ions with free radicals. J Am Chem Soc 100:3922–3926

Fogarty RV, Tobin JM (1996) Fungal melanins and their interactions with metals. Enzym Microb Technol 19:311–317

Fomina M, Gadd GM (2003) Metal sorption by biomass of melanin producing fungi grown in clay containing medium. J Chem Technol Biotechnol 78:23–34

Gadd GM, Rome L (1988) Biosorption of copper by fungal melanin. Appl Microbiol Biotechnol 29:610–617

Garty J, Garty-Spitz RL (2011) Neutralization and neoformation: analogous processes in the atmosphere and in lichen thalli—a review. Environ Exp Bot 70:67–79

Gauslaa Y, McEvoy M (2005) Seasonal changes in solar radiation drive acclimation of the sun-screening compound parietin in the lichen *Xanthoria parietina*. Basic Appl Ecol 6:75–82

Giordani P, Modenesi P, Tretiach M (2003) Determinant factors for the formation of the calcium oxalate minerals, weddellite and whewellite, on the surface of foliose lichens. Lichenologist 35: 255–270

Godinho RM, Wolterbeek HT, Pinheiro MT, Alves LC, Verburg TG, Freitas MC (2009) Micro-scale elemental distribution in the thallus of *Flavoparmelia caperata* transplanted to polluted site. J Radioanal Nucl Ch 281:205–210

Goyal R, Seaward MRD (1982) Metal uptake in terricolous lichens. III. Translocation in the thallus of *Peltigera canina*. New Phytol 90:85–98

Haselwandter K, Winkelmann G (2007) Siderophores of symbiotic fungi. In: Varma A, Chincholkar SB (eds) Microbial siderophores, soil biololgy, 12. Springer, Berlin Heidelberg, pp 91–103

Hauck M, Huneck S (2007) Lichen substances affect metal adsorption in *Hypogymnia physodes*. J Chem Ecol 33:219–223

Hauck M, Runge M (2002) Stemflow chemistry and epiphytic lichen diversity in dieback-affected spruce forest of the Harz Mountains, Germany. Flora 197:250–261

Honegger R (1993) Developmental biology of lichens. New Phytol 125: 659–677

Huneck S, Yoshimura I (1996) Identification of lichen substances. Springer, Berlin Heidelberg

Knops JMH, Nash TH, Boucher VL, Schlesinger WH (1991) Mineral cycling and epiphytic lichens: implications at the ecosystem level. Lichenologist 23:309–321

Knops JM, Nash TH, Schlesinger WH (1996) The influence of epiphytic lichens on the nutrient cycling of an oak woodland. Ecol Monogr 66: 159–179

Krog H (1982) *Punctelia*, a new lichen genus in the Parmeliaceae. Nord J Bot 2:287–292

Loppi S, Nelli L, Ancora S, Bargagli R (1997) Passive monitoring of trace elements by means of tree leaves, epiphytic lichens and bark substrate. Environ Monit Assess 45:81–88

Mafole TC, Chiang C, Solhaug KA, Beckett RP (2017) Melanisation in the old forest lichen *Lobaria pulmonaria* reduces the efficiency of photosynthesis. Fungal Ecol 29:103–110

Matee LP, Beckett RP, Solhaug KA, Minibayeva FV (2016) Characterization and role of tyrosinases in the lichen *Lobaria pulmonaria* (L.) Hoffm. Lichenologist 48:311–322

McLean J, Purvis OW, Williamson BJ, Bailey EH (1998) Role for lichen melanins in uranium remediation. Nature 391:649–650

Mikhailova IN, Sharunova IP (2008) Dynamics of heavy metal accumulation in thalli of the epiphytic lichen *Hypogymnia physodes*. Russ J Ecol 39:346–352

Muggia L, Grube M (2010) Type III polyketide synthases in lichen mycobionts. Fungal Biol 114:379–385

Nash (2008) Lichen biology. Cambridge University Press, New York

Nimis PL (2016) The lichens of Italy. A second annotated catalogue. Edizioni Università di Trieste, Trieste

Nimis PL, Andreussi S, Pittao E (2001) The performance of two lichen species as bioaccumulators of trace metals. Sci Total Environ 275: 43–51

Opanowicz M, Blaha J, Grube M (2005) Detection of paralogous polyketide synthase genes in Parmeliaceae by specific primers. Lichenologist 38:47–54

Palmqvist K (2000) Tansley review no. 117 carbon economy in lichens. New Phytol 148:11–36

Paul A, Hauck M, Fritz E (2003) Effects of manganese on element distribution and structure in thalli of the epiphytic lichens *Hypogymnia physodes* and *Lecanora conizaeoides*. Environ Exp Bot 50:113–124

Pérez-Llamazares A, Ángel Fernández J, Carballeira A, Aboal JR (2011) The sequential elution technique applied to cryptogams: a literature review. J Bryol 33:267–278

Pilas B, Sarna T, Kalyanaraman B, Swartz HM (1988) The effect of melanin on iron associated decomposition of hydrogen peroxide. Free Radical Bio Med 4:285–293

Poldini L (1989) La vegetazione del Carso isontino e triestino. Lint, Trieste

Purvis OW, Pawlik-Skowrońska B (2008) Lichens and metals. In: British mycological society symposia series. Academic Press, Cambridge, pp 175–200

Purvis OW, Bailey EH, McLean J, Kasama T, Williamson BJ (2004) Uranium biosorption by the lichen *Trapelia involuta* at a uranium mine. Geomicrobiol J 21:159–167

Richardson DHS, Shore M, Hartree R, Richardson RM (1995) The use of X-ray fluorescence spectrometry for the analysis of plants, especially lichens, employed in biological monitoring. Sci Total Environ 176:97–105

Rikkinen JK (1995) What's behind the pretty colours? A study on the photobiology of lichens. Helsinki, Finnish Bryological Society

Rinino S, Bombardi V, Giordani P, Tretiach M, Crisafulli P, Monaci F, Modenesi P (2005) New histochemical techniques for the localization of metal ions in the lichen thallus. Lichenologist 37:463–466

Saiz-Jimenez C, Shafizadeh F (1984) Iron and copper binding by fungal phenolic polymers: an electron spin resonance study. Curr Microbiol 10:281–285

Schnitzer M, Neyroud JA (1975) Further investigations on the chemistry of fungal "humic acids". Soil Biol Biochem 7:365–371

Schwertmann U (1966) Inhibitory effect of soil organic matter on the crystallization of amorphous ferric hydroxide. Nature 212:645–646

Senesi N, Sposito G, Martin JP (1987) Copper (II) and iron (III) complexation by humic acid-like polymers (melanins) from soil fungi. Sci Total Environ 62:241–252

Smith CW et al (2009) The lichens of Great Britain and Ireland. British Lichen Society, London

Solhaug KA, Gauslaa Y (1996) Parietin, a photoprotective secondary product of the lichen *Xanthoria parietina*. Oecologia 108:412–418

Solhaug KA, Gauslaa Y, Nybakken L, Bilger W (2003) UV-induction of sun-screening pigments in lichens. New Phytol 158:91–100

Swamy CT, Gayathri D, Devaraja TN, Bandekar M, D'Souza SE, Meena RM, Ramaiah N (2016) Plant growth promoting potential and phylogenetic characteristics of a lichenized nitrogen fixing bacterium, *Enterobacter cloacae*. J Basic Microbiol 56:1369–1379

Tian S, Garcia-Rivera J, Yan B, Casadevall A, Stark RE (2003) Unlocking the molecular structure of fungal melanin using ^{13}C biosynthetic labeling and solid-state NMR. Biochemistry 42:8105–8109

U.S. Environmental Protection Agency (1996) EPA-method 3052. Microwave assisted acid digestion of siliceous and organically based matrices. U.S. Government printing office, Washington DC

Wadsten T, Moberg R (1985) Calcium oxalate hydrates on the surface of lichens. Lichenologist 17:239–245

Williamson BJ, Mikhailova I, Purvis OW, Udachin V (2004) SEM-EDX analysis in the source apportionment of particulate matter on *Hypogymnia physodes* lichen transplants around the Cu smelter and former mining town of Karabash, South Urals, Russia. Sci Total Environ 322:139–154